Supporting Information of

Glycosyltransferase-Induced Morphology Transition of Glycopeptide Self-Assemblies with Proteoglycan Residues

Jing Yang,[†] Qiqige Du,[†] Long Li,[†] Tingting Wang,[‡,/] Yingle Feng,[†] Mu-Ping Nieh,[#,⊥] Juzheng Sheng,[,‡,/] and Guosong Chen[*,†,§]*

[†] The State Key Laboratory of Molecular Engineering of Polymers and Department of Macromolecular Science, Fudan University, Shanghai 200433, China.

[‡] Key Laboratory of Chemical Biology of Natural Products (Ministry of Education), Institute of Biochemical Drug, School of Pharmaceutical Science, Shandong University, Jinan 250012, China.

[/] National Glycoengineering Research Center, Shandong University, Jinan 250012, China.

[#] Polymer Program, Institute of Materials Science, University of Connecticut, Storrs, Connecticut 06269 United States.

[⊥] Department of Chemical and Biomolecular Engineering, University of Connecticut, Storrs, Connecticut 06269, United States.

[§] Multiscale Research Institute of Complex Systems, Fudan University, Shanghai 200433, China

Content

I. General information 0

II. Synthesis and characterization of compounds 3

IV. Study on Self-assembly behavior of GlcA-YF 8

V. TEM and liquid phase AFM images of morphology transition 10

VI. Characterization of GalNAcGlcA-YF and GlcNAcGlcA-YF self-assemblies. 11

VI. Cell Viability Vest 13

VII. Glycosyltransferase-induced morphology transition in cell medium 14

IX. Confocal Fluorescence Microscopy Images 15

X. NMR and MS spectrum of Synthesized Compounds 17

XI. Reference 25

I. General information

Materials.

Chemicals and solvents were purchased from J&K Chemical, TCI, Sigma-Aldrich and used without further purification. UDP-GalNAc and UDP-GlcNAc were purchased from Carbosynth China Ltd. And stored at -20°C. Plasmid used were offered by Prof. Juzheng Sheng's group in Shandong University. Anhydrous solvent used in reactions were purified by a solvent purification system (PS-MD-3, Innovative Technology Inc., USA) before using. Unless specially mentioned, all other chemicals were used as received.

Characterization.

NMR ^{1}H NMR spectra and ^{13}C NMR spectra were recorded on a 400 MHz Bruker AVANCE III HD spectrometer, and the acquired NMR data were analyzed with MestRe Nova software. Chemical shift values were referenced using the solvent peak at DMSO-d_6 (2.50), D_2O (4.80) or MeOD (3.31).

Matrix-assisted laser desorption ionization time-of-flight mass spectrometry (MALDI-TOF MS) MALDITOF MS measurement was performed using AB SCIEX MALDI-TOF/TOF MS 5800 System, using DHB or DCTB as matrix in reflection mode.

High Performance Liquid Chromatography (HPLC) HPLC data were measured on Waters instrument equipped with 1525 binary HPLC pump, 2489 UV/Visible detector and 2414 Refractive index detector.

Dynamic light scattering (DLS) The hydrodynamic diameters of glyco-nanoparticles were measured by dynamic light scattering (DLS) (Malvern Zeta-sizer Nano ZS90). All sample solutions were filtered through Millipore filters (220 nm) to remove the dust and kept at 25°C.

Fluorescence emission spectroscopy Fluorescence spectrums were conducted on a Steady state/transient fluorescence spectrograph (QM40) of PFI.

Transmission electron microscopy (TEM) TEM images were taken with a Tecnai G2 instrument operating at an accelerating voltage of 200 KV or High Contrast TEM instrument operating at an accelerating voltage of 120 KV. TEM samples were prepared by depositing a drop of the sample solution (1 mg/mL, 3 μL) on the copper grid for several seconds. Then the solution was blotted away and 3 μL of 1 wt% uranyl acetate solution was dropped to stain the particles for about 40 seconds. TEM images were analyzed by ImageJ software, and more than 150 nanoparticles (the stained samples) were counted for each sample to obtain the area or length information.

Atomic Force Microscope (AFM) Gaseous phase AFM was operated on a Bruker Multimode VIII SPM equipped with a J scanner. Experiments were performed in tapping mode with RTESPA-300 tip (spring constant 40 N/m, Bruker). Sample solution (10 μL) was deposited on freshly cleaved mica under dry condition and kept for about 10 s before blotting away. **Liquid phase AFM** was detected in the same instrument. 30 μL solution of nanofibers was added into the liquid cell and incubated for 5 min, following with the addition of 1.05 eq. donor, 10 μL GTs, Tris-HCl (pH = 7.23) and $MnCl_2$ to guarantee the final concentration was 20 mM.

Confocal laser-scanning microscopy (CLSM) CLSM images of RAW 264.7 macrophages were obtained using confocal microscopy (Nikon C^{2+}) with excitation wavelength at 488 nm for fluorescein or 561 nm for Dil. Fluorescence images were analyzed under NIS-Elements Viewer software (Nikon). Images were analyzed under NIS-Elements Viewer software (Nikon). Representative images are selected from one of three independent experiments.

Circular dichroism spectrum (CD) CD spectra was taken by a Chirascan instrument (Applied Photophysics) with a 1 mm cuvette.

Solution-phase synchrotron small angle X-ray scattering (SAXS) SAXS experiment data were obtained on the SAXS beam line (BL16B1) of Shanghai Synchrotron Radiation Facility (SSRF). Scattering images recorded were integrated along the Debye-Scherrer ring using the FIT2D software.

Glycopeptide self-assembly for nanofibers prepration. GlcA-YF was dissolved in water at the concentration of 1 mg/mL after sonication for 10 min and stayed at room temperature.

Morphology transition in water. 1 mL nanofibers were incubated with 1.05 eq. donor in mixed solution of Tris-HCl (pH = 7.23, 20 mM), $MnCl_2$ (20 mM) and 300 μL purified GTs at 37°C. The reaction conversion in monomeric state was detected by HPLC and the microscale morphology was monitored by TEM.

Glycopeptide self-assembly directly. Purified **GalNAcGlcA-YF** or **GlcVAcGlcA-YF** was dissolved in water at the concentration of 1 mg/mL after sonication for 10 min and stayed at room temperature.

Co-assembly of GlcA-YF and FITC-YF. GlcA-YF was co-assembled with 1 wt% of **FITC-YF** at a concentration of 1 mg/mL. 10 μL 0.1 M Na_2CO_3 solution was added at first to help the solvation of **FITC-YF** and sonicated for 10 min for dissolving completely. Then 20 μL 0.1 M HCl was added to the solution to accelerate the formation of FITC labelled nanofibers. Long nanofibers could be observed 5 h later.

Cytotoxicity evaluation using cell counting kit-8 (CCK-8) assay. RAW264.7 macrophage cell line was cultured in a complete culture RPMI 1640 medium, supplemented with 10% fetal bovine serum (GIBCO) and 1% antibiotic antimycotic solution (GIBCO) at 37°C and 5% CO_2 condition. In the cell viability experiments, RAW264.7 cells were cultured in 96 wells plate overnight, then glyco-assemblies were added into culture medium at varied concentrations for 24 h. Cell viability in response to glyco-assemblies as analyzed by CCK-8 assay (Dojindo) following the manufacturer's procedures. Generally, cell supernatant was removed and was washed with PBS for three times. CCK-8 reagent was added into wells in a ratio of 1/10 in culture medium. Cells were cultured in an incubator for 1 to 4 h. Finally, the plate was read with Microplate Reader (BioTex ELx800) in 450 nm.

Cell interaction assay. RAW264.7 macrophage cell line was cultured in a complete culture RPMI 1640 medium, supplemented with 10% fetal bovine serum (GIBCO) and 1% antibiotic antimycotic solution (GIBCO) at 37°C and 5% CO_2 condition. Then 200 μL FITC-labeled nanofibers was added to active RAW 264.7 macrophages, following with the addition of 3 μL donor (100 mM), 10 μL $MnCl_2$, and 50 μL GTs. After incubation for 12 h at 37°C, cells were washed with PBS to remove culture medium and fixed with 4% paraformaldehyde for 10 min. The cell membrane was stained with 3 μM Dil (DiIC18(3)) for 10 min and washed with PBS. Fluorescence images of RAW 264.7 macrophages were obtained using confocal laser-scanning microscopy.

Transwell assay. The transwell chamber was infiltrated with PBS buffer and placed into a 24-well culture plate. At the same time, RAW 264.7 macrophages in logarithmic growth phase were adjusted with 0.1% bovine serum albumin (BSA) serum-free DMEM culture medium. 100 μL cells were seeded into the transwell upper chamber with three replicates in each group. In the lower chamber, 500 μL serum-free DMEM culture medium with glycol-assemblies (100 μg/mL) and 0.1% BSA were added. Taking 500 μL of

DMEM culture medium of 10% fetal bovine serum as the positive control and 500 μL serum-free DMEM culture medium containing 0.1% BSA as the negative control. Cells were incubated at 37°C and 5% CO_2 condition for 12 h. Cells were washed with pre-chilled PBS at 4°C for several times and fixed with 4% paraformaldehyde for 10 min and stained Giemsa for 15 min. The number of migrating cells was recorded under microscope and analyzed by Prism 6.

Examination of catalyzing efficiency of KfoC and PmHS2. 0.06 mM donor (UDP-GalNac for KfoC; UDP-GlcNAc for PmHS2) and 0.04 mM **GlcA-YF** were added to 0.4 mL buffer with 20 mM Tris-HCl (PH = 7.23) and 20 mM $MnCl_2$. The enzyme (0.1 mL, C = 0.8 mg/mL, $A_{280/260}$ = 0.6) was added and the solution and incubated for 4 hat 37°C. The reaction was quenched by boiling at 90°C for 2 min following with the analysis by HPLC at 245 nm to demonstrate the formation of disaccharide and reaction conversion. The column (YMC-Triant C_{18}) was eluted with a mixture of MeOH (HPLC grade, Sigma Chemical) and ultra-pure water (with 0.1% TFA) with the ratio of 2/1 at a flow rate of 1.0 mL/min.

Expression and Purification of KfoC and PmHS2. KfoC (GeneBank accession number: AB079602), one of the chondroitin polymerases was recombinant expressed in BL21(DE3) cells as a soluble N-His_6-tagged fusion protein. The plasmid was transferred into *E. coli* BL21(DE3) to give the recombinant strain, BL21-KfoC. The recombinant strain was cultured in Lysogeny broth (LB) medium supplemented with 100 μg/mL kanamycin at 37°C until the OD_{600} value reached 0.6 to 0.8, followed by treatment with 0.2 mM isopropyl-1-thio-β-D-galactopyranoside (IPTG) for 18 h at 20°C to induce the expression of KfoC. Then the cells were centrifuged and broken by low-temperature and high-pressure sterilize. The protein was purified over a Ni-Sepharose 6 Fast-Flow column (GE healthcare life sciences, Pittsburgh, PA, USA). The protein purity was analyzed by 10% SDS-PAGE stained with Coomassie Blue and concentrate was detected by Nanodrop A_{280}.

PmHS2 (GenBank accession number: AAQ55110), one of the heparin polymerases was expressed and purified as described above.

II. Synthesis and characterization of compounds

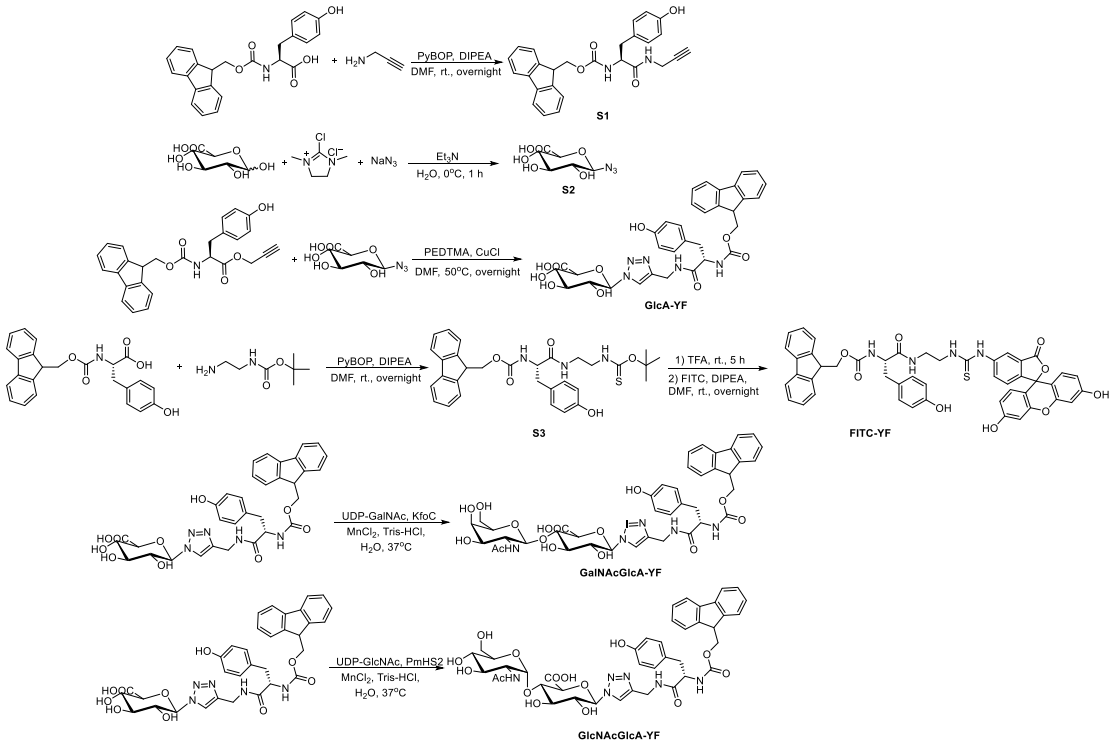

Scheme S1. Synthetic routes and chemical structures of compounds.

Synthesis of **S1**. N-fluorenylmethoxycarbonyl L-tyrosine (YF, 2.01 g, 4.99 mmol) was added to a 100 mL round bottom flask, following with the addition of dry DMF (35 mL) under Ar atmosphere. Then benzotriazol-1-yl-oxytripyrrolidinophosphonium hexafluorophosphate (PyBOP, 3.11 g, 5.98 mmol), N, N-Diisopropylethylamine (DIPEA; 0.7 mL, 5.98 mmol) and propargyl amine (0.68 mL, 9.98 mmol) was added slowly in an ice bath. After stirring for 30 min, the solution was removed to room temperature stirring overnight. TLC (ethylacetate/petroleum ether = 2/1) indicated the formation of a product with complete consumption of the starting material. The reaction mixture was concentrated under reduced pressure and extracted with water and ethylacetate. The organic layer was dried with $MgSO_4$, filtered and concentrated in vacuo. Recrystallisation from methanol and dichloromethane gave the product **S1** as white solid (1.98 g, yield: 90 %).

^{1}H NMR (400 MHz, DMSO-d_6) δ 7.88 (d, J = 7.6 Hz, 2H), 7.67 - 7.62 (m, 2H), 7.43 - 7,38 (m, 2H), 7.36 - 7.24 (m, 2H), 7.08 (d, J = 8.4 Hz, 2H), 6.64 (d, J = 8.4 Hz, 2H), 4.24 - 4.04 (m, 4H), 3.95 - 3.80 (m, 2H), 3.13 (t, J = 1.6 Hz, 1H), 2.92 - 2.75 (m, 1H), 2.66 (dd, J = 10.4, 3.2 Hz, 1H). **^{13}C NMR** (100 MHz, DMSO-d_6) δ 171.54, 155.86, 143.90, 143.82, 140.75, 130.24, 128.18, 127.72, 127.16, 125.47, 125.40, 120.17, 114.94, 81.09, 73.24, 65.74, 56.53, 46.65, 36.82, 28.11.

Synthesis of **S2**. **S2** was synthesized as described in the literature [1]. In brief, D-glucuronic acid (GlcA; 0.50 g, 2.58 mmol) and NaN_3 (1.51 g, 23.18 mmol) was added to water (13 mL) in an ice bath following with the addition of triethylamine (Et_3N; 3.1 mL, 23.18 mmol) dropwise. Then the 2-chloro-1,3-dimethylimidazolium chloride (DMC; 1.31 g, 7.73 mmol) was added slowly. The mixture was stirred for 1 h at 0°C. TLC (methanol/dichloromethane = 1/2) indicated the formation of product. After collection by reduced pressure, ethanol was added and the solid could be collected through filter. Washing the solid with DMF and the product was dissolved. After filtering and concentrating in vacuo, the residue could be purified

by flash column chromatography (methanol/dichloromethane = 1/2) to give the product **S2** as white solid (0.48 g, yield: 85%).
^{1}H NMR (400 MHz, D_2O) δ 4.75 (d, *J* = 8.8 Hz, 1H), 3.82 (d, *J* = 8.4 Hz, 1H), 3.59 - 3.48 (m, 2H), 3.31 (t, *J* = 8.8 Hz, 1H).

Synthesis of **GlcA-YF**. The product was given under the traditional "Click" reaction. Briefly, **S1** (0.48 g, 1.13 mmol) and **S2** (0.21 g, 0.94 mmol) were dissolved in DMF (11.3 mL). The reaction mixture was allowed to stir around 15 min with bubbling of argon. Cuprous chloride (18.6 mg, 0.19 mmol) and pntamethyldiethylenetriamine (PEDTMA; 39 μL, 0.19 mmol) was added and bubbled for another 15 min. The solution was stirred at 50°C overnight. TLC (methanol/dichloromethane = 1/3) indicated the formation of product. After concentration under reduced pressure, the residue could be purified by flash column chromatography (methanol/dichloromethane = 1/3) as light brown powder (0.50 g, yield: 80%). Additionally, the product could be further purified by HPLC (column: YMC-Triart C_{18} column (250 × 20.0 mml. D.); low rate: 10 mL/min; eluent: methanol/water (0.1% TFA) = 2/1).
^{1}H NMR (400 MHz, MeOD) δ 7.79 (s, 1H), 7.78 (d, *J* = 2.8 Hz, 2H), 7.63 - 7.56 (m, 2H), 7.37 (q, *J* = 7.6 Hz, 2H), 7.33 - 7.27 (m, 2H), 7.02 (d, *J* = 8.0 Hz, 2H), 6.69 (d, *J* = 9.2 Hz, 2H), 5.62 (d, *J* = 9.3 Hz, 1H), 4.47 - 4.37 (m, 3H), 4.32 - 4.23 (m, 2H), 4.20 - 4.09 (m, 2H), 4.04 - 3.94 (m, 1H), 3.73 (t, *J* = 9.2 Hz, 1H), 3.64 - 3.56 (m, 1H), 2.98 (dd, *J* = 14.0, 7.2 Hz, 1H), 2.80 (dd, *J* = 13.6, 8.4 Hz, 1H). **^{13}C NMR** (100 MHz, MeOD) δ 157.20, 157.02, 145.11, 145.02, 142.37, 131.21, 128.88, 128.71, 128.56, 127.98, 126.06, 125.98, 123.31, 120.68, 116.13, 89.06, 89.04, 89.02, 87.95, 78.88, 78.80, 77.75, 73.85, 73.17, 67.70, 66.99, 58.03, 35.52. **MALDI-TOF MS** calculated for $C_{33}H_{33}N_5O_{10}$ $[M - H]^-$: 658.64, found: 658.75.

Synthesis of **S3**. **S1** (1.00 g, 2.50 mmol) was added to a 50 mL round bottom flask, following with the addition of dry DMF (17.5 mL) under Ar atmosphere. Then PyBOP (1.56 g, 2.99 mmol), DIPEA (0.35 mL, 2.99 mmol) and t-butyl (2-aminoethyl) carbamate (0.48 g, 3.00 mmol) was added slowly in an ice bath. After stirring for 30 min, the solution was moved to room temperature stirring for overnight. TLC (ethylacetate/petroleum ether = 1/2) indicated the formation of a product with complete consumption of the starting material. The reaction mixture was concentrated under reduced pressure and the extracted with water and ethylacetate. The organic layer was dried with $MgSO_4$, filtered and concentrated in vacuo. The product **S3** was purified by column chromatography as white solid (1.25 g, yield: 92 %).
^{1}H NMR (400 MHz, DMSO-d_6) δ 7.86 (d, *J* = 7.6 Hz, 2H), 7.72 (d, *J* = 8.0 Hz, 1H), 7.65 (t, *J* = 7.6 Hz, 1H), 7.39 (m, 2H), 7.30 (dt, *J* = 15.4, 7.6 Hz, 2H), 7.08 (d, *J* = 10.4 Hz, 2H), 6.67 (d, *J* = 8.4 Hz, 2H), 4.26 - 4.11 (m, 4H), 3.16 (dt, *J* = 11.8, 6.0 Hz, 1H), 3.13 - 3.03 (m, 1H), 3.00 (t, *J* = 5.6 Hz, 2H), 2.91 - 2.86 (m, 1H), 2.71 (dd, *J* = 13.4, 10.2 Hz, 1H), 1.36 (s, 9H). **^{13}C NMR** (100 MHz, DMSO-d_6) δ 171.97, 155.60, 155.98, 155.90, 144.00, 143.95, 140.89, 130.36, 128.39, 128.06, 127.86, 127.56, 127.29, 125.57, 125.48, 124.78, 120.27, 119.31, 115.11, 109.83, 77.99, 65.86, 56.84, 46.82, 37.12, 28.41. **MALDI-TOF MS** calculated for $C_{31}H_{35}N_3O_6$ $[M + Na]^+$: 568.24, found: 568.21.

Synthesis of **FITC-YF**. **S3** (1.00 g, 1.83 mmol) was dissolved in 3.7 mL dry DCM following with the addition of TFA (HPLC grade, 0.81 mL, 9.15 mmol) dropwise. The mixture reacted at room temperature for 5 h. TLC (ethylacetate/petroleum ether = 1/2) indicated the deprotection of Boc group completely. Then the reaction mixture was concentrated under reduced pressure to remove the by-products. Next, FITC (0.86 g, 2.20 mmol) was added and dissolved by 18.3 mL dry DMF under Ar atmosphere, following with the addition of DIPEA (0.39 mL, 2.20 mmol) dropwise. The reaction mixture reacted at room temperature overnight. TLC (ethylacetate/petroleum ether = 1/1) indicated the formation of a product and purified

with column chromatography to get orange solid (1.07 g, yield: 70%).

^{1}H NMR (400 MHz, DMSO-d_6) δ 7.87 (d, *J* = 7.6 Hz, 2H), 7.74 (d, *J* = 8.0 Hz, 1H), 7.64 (t, *J* = 8.4 Hz, 2H), 7.51 (d, *J* = 8.8 Hz, 1H), 7.42 - 7.38 (m, 2H), 7.30 (m, 2H), 7.17 (d, *J* = 8.0 Hz, 1H), 7.06 (d, *J* = 8.0 Hz, 2H), 6.79 - 6.45 (m, 8H), 4.25 - 4.09 (m, 4H), 3.68 - 3.52 (m, 2H), 2.96 - 2.83 (m, 1H), 2.80 - 2.61 (m, 1H). **^{13}C NMR** (100 MHz, DMSO-d_6) δ 172.15, 168.60, 162.48, 159.59, 155.85, 151.98, 143.83, 140.75, 130.20, 129.13 , 128.25, 127.71, 127.14, 125.47, 125.37, 120.17, 114.94, 112.69, 109.81, 102.33, 99.62, 65.70, 56.72, 46.67, 43.66, 43.63, 37.91, 36.98, 35.88. **MALDI-TOF MS** calculated for $C_{47}H_{38}N_2O_9S$ $[M + H]^+$: 835.90, found: 835.82.

Synthesis of **GalNAcGlcA-YF.** The synthesis of **GalNAcGlcA-YF** and **GlcNAcGlcA-YF** was according to the procedures of previous literature [2]. **GlcA-YF** (14.1 mg, 0.022 mmol) and UDP-GalNAc (14.6 mg, 0.023 mmol) was dissolved in 100 mL buffer with 20 mM Tris-HCl (PH = 7.23) and 20 mM $MnCl_2$, following with the addition of 5 mL freshly prepared KfoC (C = 0.9 mg/mL, $A_{260/280}$ = 0.6). The mixture was treated at 37°C overnight. HPLC analysis suggested the complete conversion of **GlcA-YF**. The reaction mixture was concentrated under reduced pressure and purified by preparative HPLC (YMC-Actus Triart C_{18}, 250*20.0 mm) eluted with H_2O (with 0.1% TFA)/MeOH (1/2, v/v) at a flow rate of 10.0 mL/min. The purity of **GalNAcGlcA-YF** was examined by catalytic HPLC.

^{1}H NMR (400 MHz, DMSO-d_6) δ 8.01 (s, 1H), 7.88 (d, *J* = 7.6 Hz, 2H), 7.70 - 7.60 (m, 2H), 7.37 - 7.44 (m, 2H), 7.36 - 7.26 (m, 2H), 7.13 - 7.00 (m, 2H), 6.63 (d, *J* = 8.0 Hz, 2H), 5.76 (d, *J* = 9.6 Hz, 1H), 5.65 (d, *J* = 5.2 Hz, 1H), 5.11 (s, 1H), 4.81 - 4.54 (m, 4H), 4.40 - 4.32 (m, 2H), 4.22 - 4.10 (m, 3H), 3.94 - 3.84 (m, 2H), 3.71 - 3.62 (m, 2H), 3.46 (t, *J* = 5.2 Hz, 2H), 2.88 (d, *J* = 10.0 Hz, 1H), 2.67 (d, *J* = 15.6 Hz, 1H), 1.81 (s, 3H). **MALDI-TOF MS** calculated for $C_{41}H_{46}N_6O_{15}$ $[M - H]^-$: 861.85, found: 861.85

Synthesis of **GlcNAcGlcA-YF. GlcA-YF** (19.1 mg, 0.029 mmol) and UDP-GlcNAc (14.6 mg, 0.030 mmol) was dissolved in 145 mL buffer with 20 mM Tris-HCl (PH =7 .23) and 20 mM $MnCl_2$, following with the addition of 7 mL freshly prepared KfoC (C = 0.8 mg/mL, $A_{260/280}$ = 0.7). The mixture was treated at 37°C overnight. HPLC analysis suggested the complete conversion of **GlcA-YF**. The reaction mixture was concentrated under reduced pressure and purified by preparative HPLC (YMC-Actus Triart C_{18}, 250*20.0 mm) eluted with H_2O (with 0.1% TFA)/MeOH (1/2, v/v) at a flow rate of 10.0 mL/min.

^{1}H NMR (400 MHz, DMSO-d_6) δ 7.92 (s, 1H), 7.81 (d, *J* = 7.6 Hz, 1H), 7.68 (d, *J* = 4.4 Hz, 1H), 7.54 (dd, *J* = 7.6, 3.0 Hz, 2H), 7.42 - 7.33 (m, 1H), 7.32 - 7.20 (m, 2H), 7.00 (d, *J* = 4.0 Hz, 2H), 6.61 (d, *J* = 9.2 Hz, 2H), 5.62 (d, *J* = 4.8 Hz, 1H), 5.12 (d, *J* = 3.2 Hz, 1H), 4.36 - 4.29 (m, 1H), 3.88 - 3.79 (m, 6H), 3.77 - 3.64 (m, 3H), 3.63 - 3.47 (m, 1H), 3.46 - 3.34 (m, 1H), 3.32 - 3.26 (m, 2H), 2.90 - 2.83 (m, 2H), 2.68 - 2.58 (m, 2H), 1.86 (s, 3H). **MALDI-TOF MS** calculated for $C_{41}H_{46}N_6O_{15}$ $[M - H]^-$: 861.85, found: 861.97.

III. Examination of chemoenzymatic reaction.

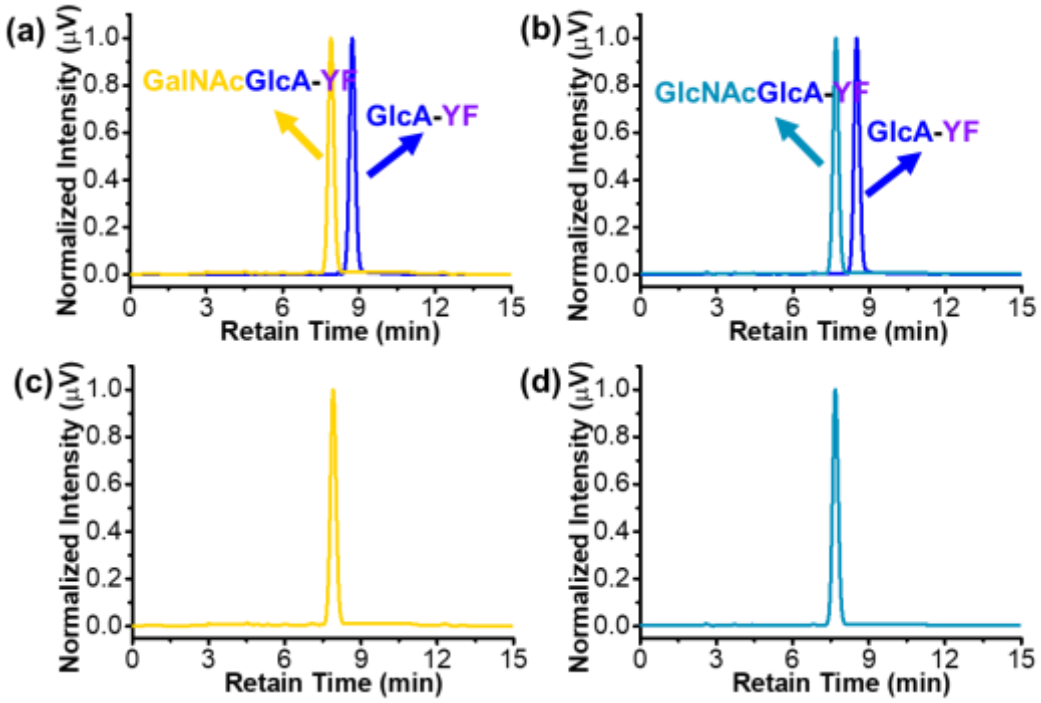

Figure S1. Examination of chemoenzymatic reaction taking **GlcA-YF** as acceptor. HPLC graphs of (a) **GalNAcGlcA-YF** and **GlcA-YF** separation; (b) **GlcNAcGlcA-YF** and **GlcA-YF** separation; (c) purified **GalNAcGlcA-YF**; (d) purified **GlcNAcGlcA-YF**.

IV. Study on Self-assembly behavior of GlcA-YF

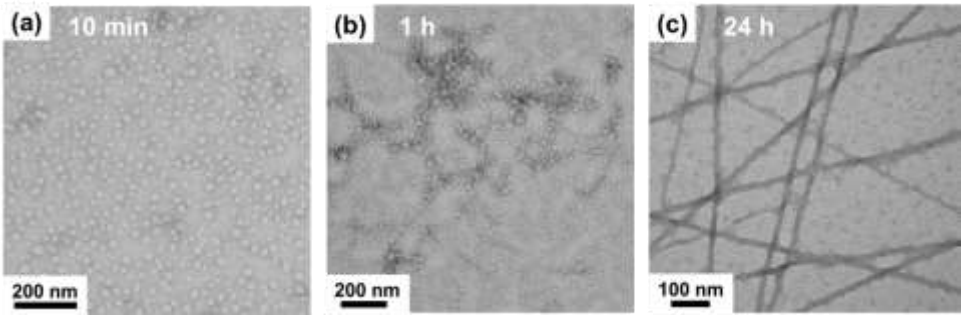

Figure S2. TEM micrographs of time-dependent self-assembly process of **GlcA-YF**.

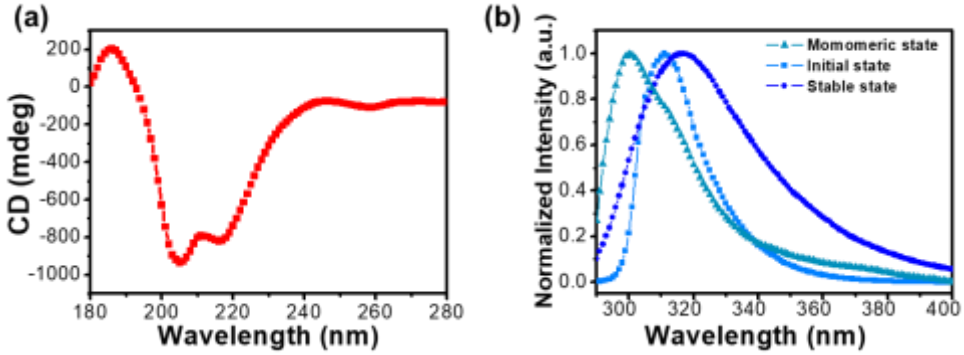

Figure S3. Micro-scale characterization of nanofibers assembled by **GlcA-YF**. (a) CD spectrum; (b) concentrate-dependent fluorescence spectrum.

Small-angle X-ray Scattering (SAXS) Data Analysis

The SAXS data of **GLcA-YF** nanofibers were best fit with core-shell cylindrical model, $P_{csc}(q)$, where the inner radius, the shell thickness and the length of the cylinder can be represented as R, t and L, respectively as shown in the inset of Figure S3. The SAXS intensity, $I(q)$ can be expressed as

$$P_{CSC}(q) = V_{shell}\int_0^1 \Psi^2[q,(R+t)(1-x^2)^{1/2},R(1-x^2)^{1/2}]\left(\frac{sin\frac{qLx}{2}}{\frac{qLx}{2}}\right)^2 dx,$$

where

$V_{shell} = \pi\left[(R+t)^2 - R^2\right]L,$

$\Psi[q,Y,Z] = \frac{2(R+t)^2}{(R+t)^2-R^2}\left[\frac{J_1(qY)}{qY} - \left(\frac{R}{R+t}\right)^2\frac{J_1(qZ)}{qZ}\right],$

$J_1(a) = \frac{sin(a)-a\cdot cos(a)}{a^2}$, the first order Bessel function, and ϕ and $\Delta\rho$ are the volume fraction of the core-shell cylinders and electron density difference between water and **GLcA-YF**. It should be noted that L is larger than the attainable length range in the current scattering configuration. We cannot accurately obtain the reliable length of the cylinders. Throughout the best fitting procedure, the R is assumed to follow Schulz distribution function with a polydispersity of $\sigma_R/\langle R\rangle$, where σ_R and $\langle R\rangle$ represent the standard deviation and average of R, respectively. The best fit agrees well with the SAXS data as shown in Figure S3. The best

fit R and *t* are 13.98 and 23.15 Å, respectively.

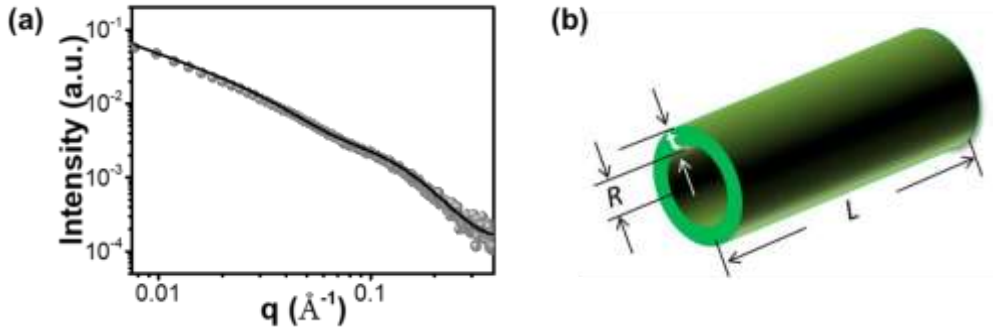

Figure S4. (a) The SAXS data (symbols) and its best fit (solid curve) using core-shell cylindrical model; (b) SAXS model used in this system.

V. TEM and liquid phase AFM images of morphology transition

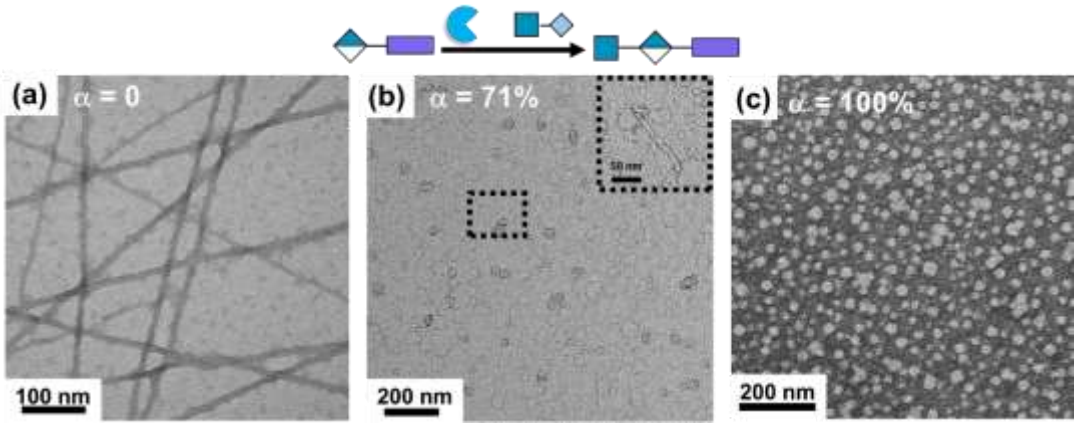

Figure S5. TEM micrographs of morphology transition with **GlcNAcGlcA-YF** generation *in situ* in different reaction conversion (a) α = 0; (b) α = 71% (inset: TEM image of nanofiber fragments at a higher magnification); (c) α = 100%.

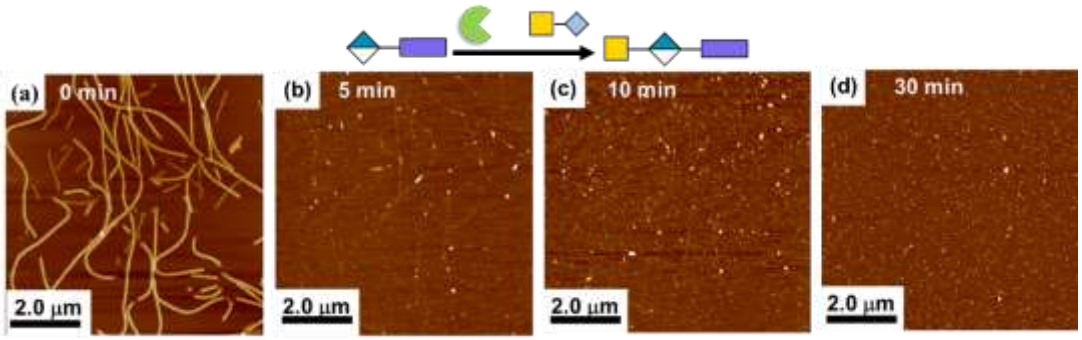

Figure S6. Liquid phase AFM micrographs with **GalNAcGlcA-YF** generation in situ at (a) 0; (b) 5; (c) 10; (d) 30 min.

VI. Characterization of GalNAcGlcA-YF and GlcNAcGlcA-YF Self-assemblies.

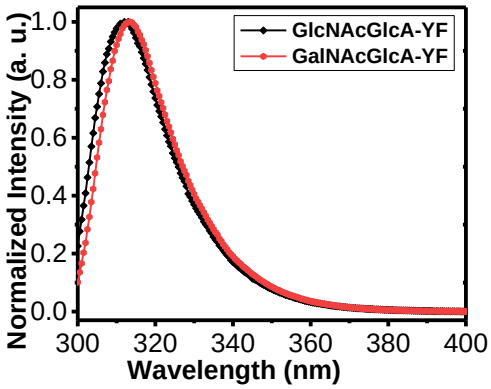

Figure S7. Fluorescence spectrum of **GalNAcGlcA-YF** (red line) and **GlcNAcGlcA-YF** (black line) assemblies in solution.

VI. Cell Viability Vest

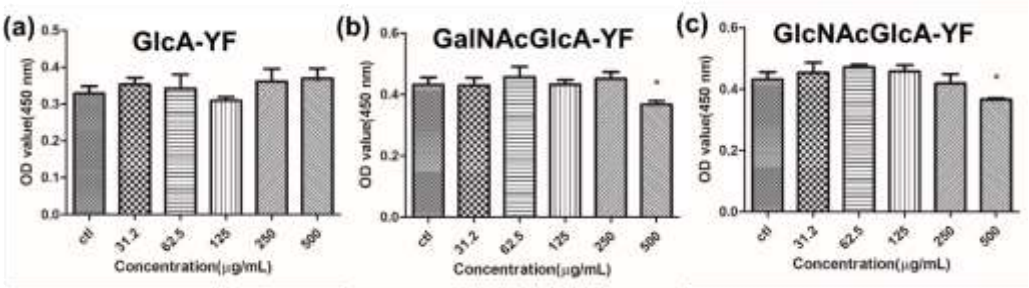

Figure S8. Cell viability of (a) **GlcA-YF**, (b) **GalNAcGlcA-YF** and (c) **GlcNAcGlcA-YF** assemblies at different concentration.

VII. Glycosyltransferase-induced morphology transition in cell medium

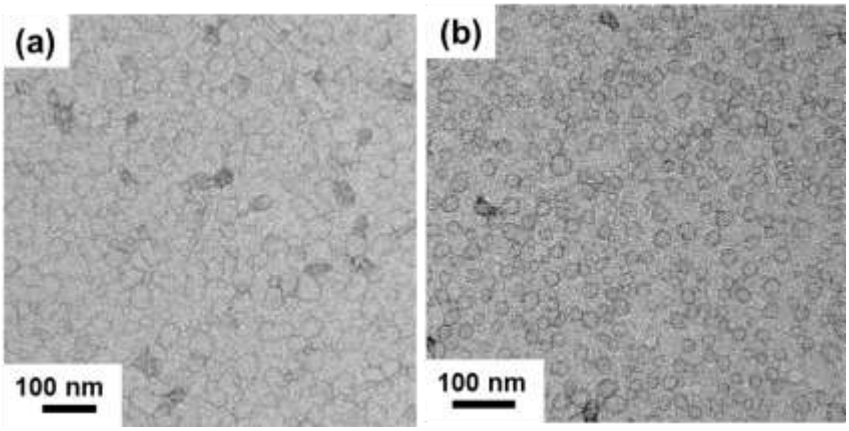

Figure S9. TEM images of (a) **GalNAcGlcA-YF** and (b) **GlcNAcGlcA-YF** (b) nanoparticles generated in cell medium in situ.

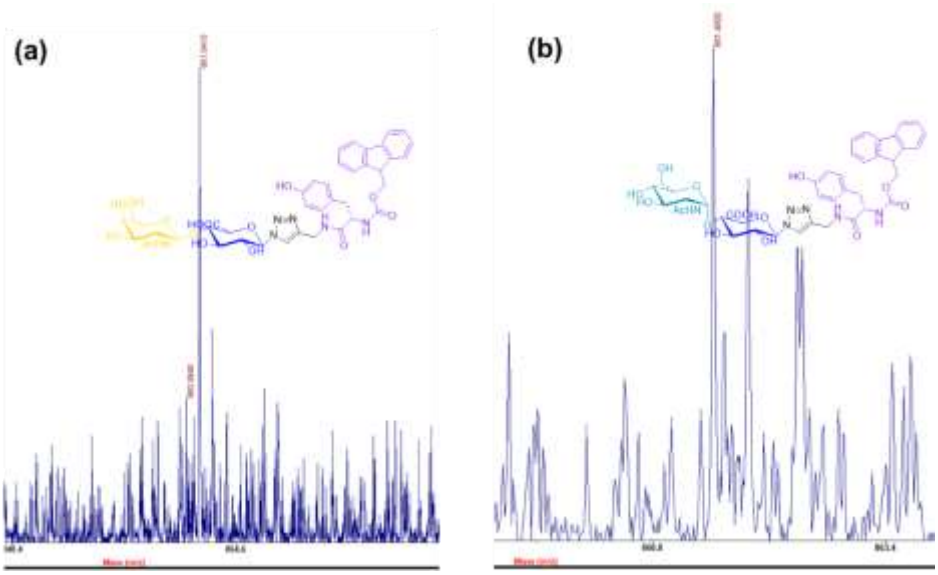

Figure S10. MALDI-TOF MS spectra of (a) **GalNAcGlcA-YF** generation; (b) **GlcNAcGlcA-YF** generation incubated with RAW 264.7 cells in cell medium.

IX. Confocal Fluorescence Microscopy Images

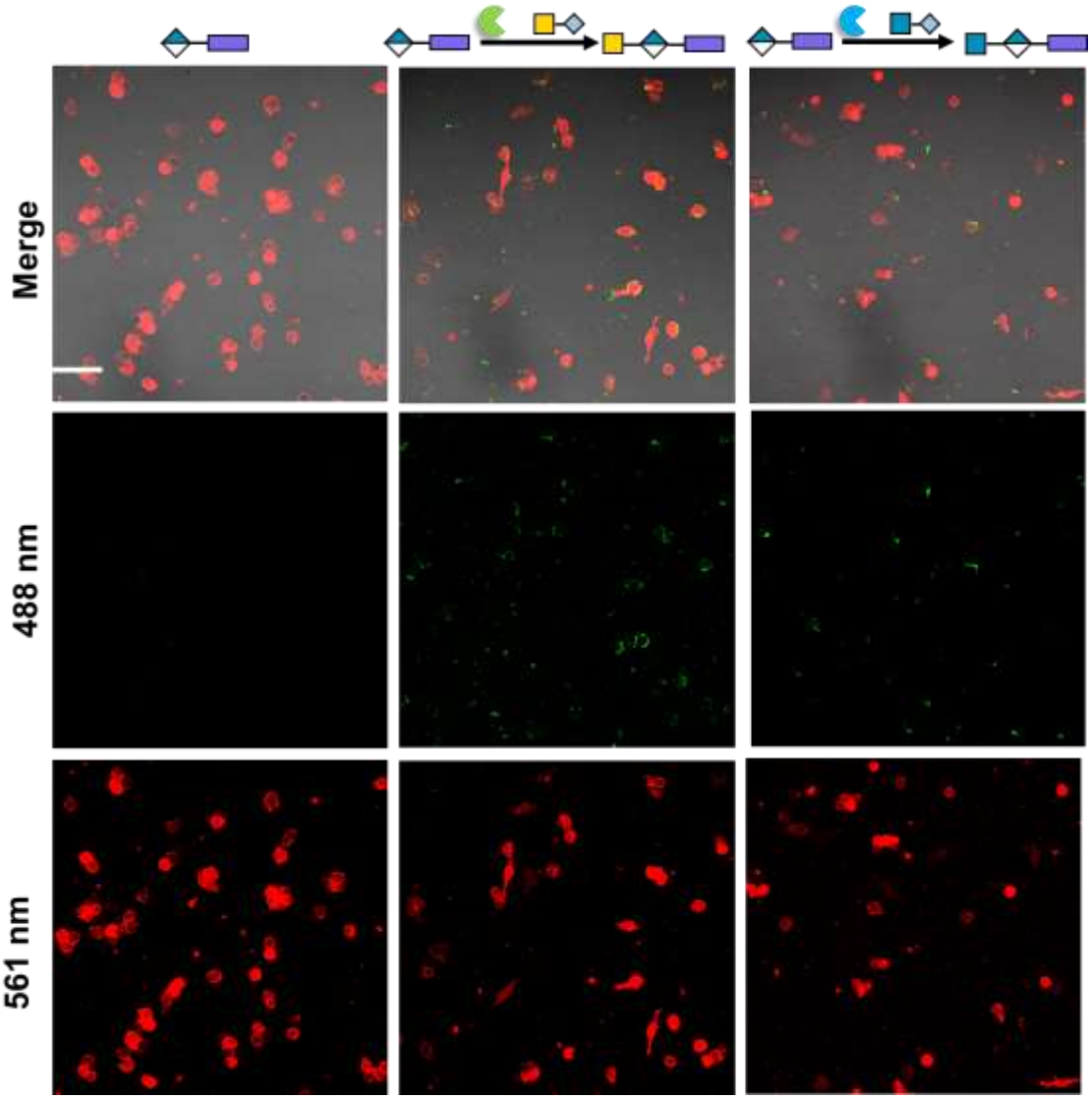

Figure S11. Confocal fluorescence micrographs of cell incubated with nanofibers assembled by **GlcA-YF** (the first column); **GalNAcGlcA-YF** generation in situ (the second column); **GlcNAcGlcA-YF** generation in situ (the third column) (Scale bar = 100 μm).

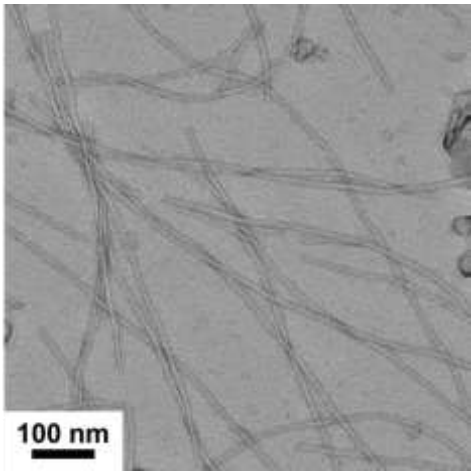

Figure S12. TEM image of coassemblies of **GlcA-YF** and **FITC-YF**.

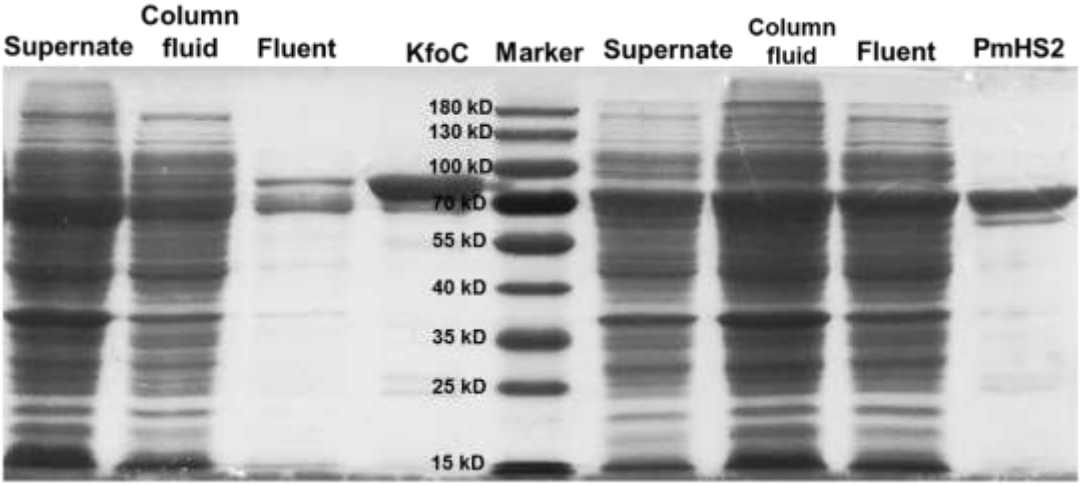

Figure S13. SDS-PAGE of purified KfoC and PmHS2

X. NMR and MS spectrum of Synthesized Compounds

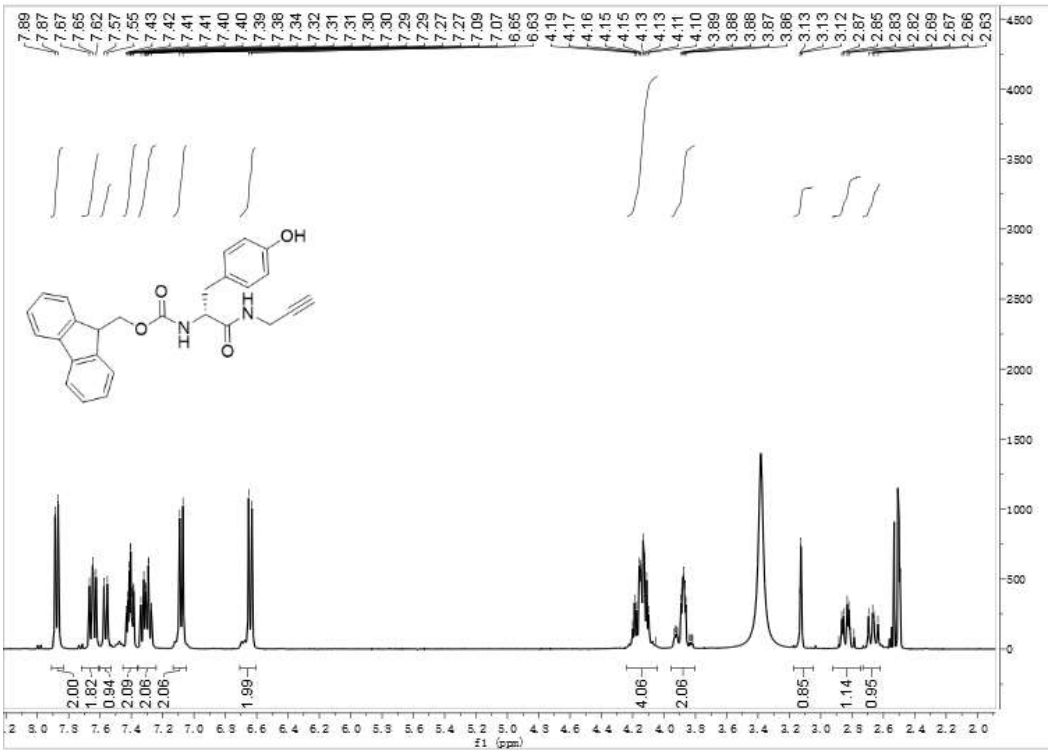

Figure S14. ^{1}H NMR spectrum of **S1** (DMSO-d_6, 400 Hz).

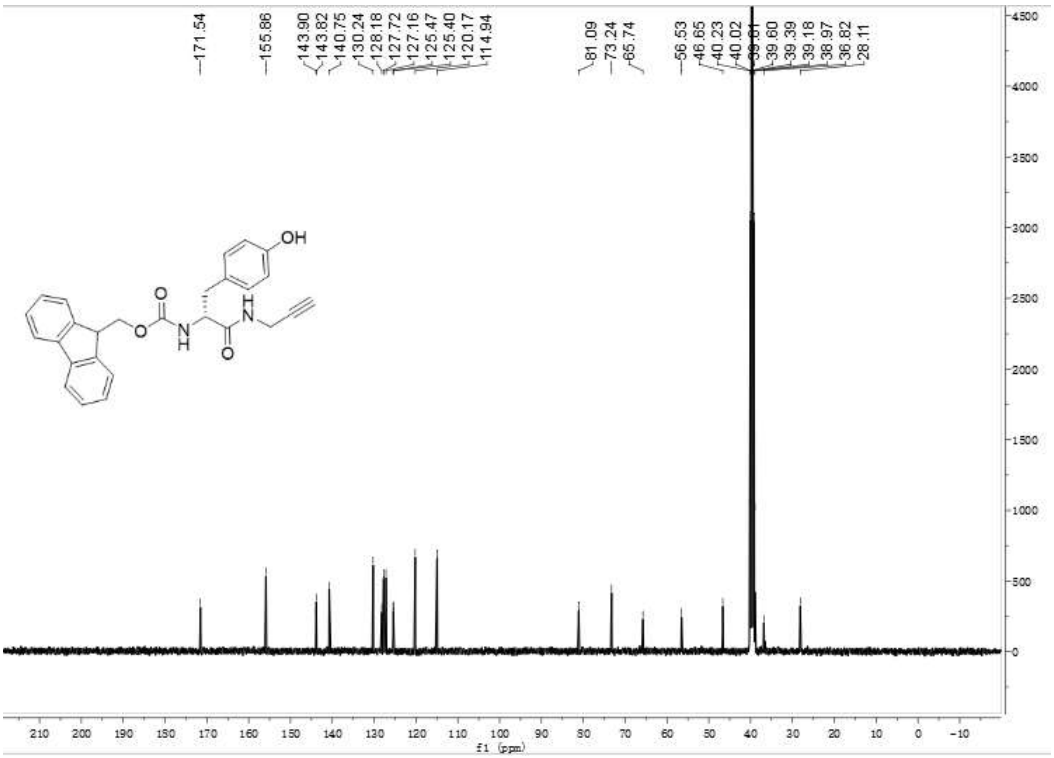

Figure S15. ^{13}C NMR spectrum of **S1** (DMSO-d_6, 100 MHz).

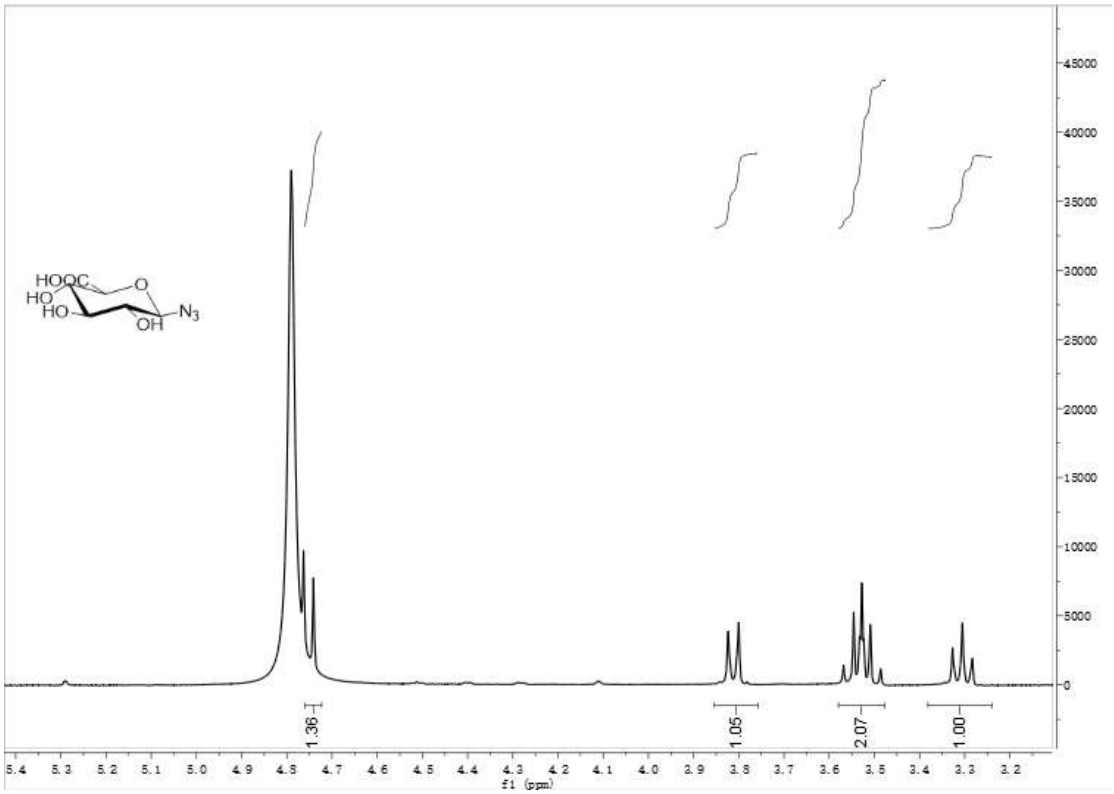

Figure S16. ^{1}HNMR spectrum of **S2** (D_2O, 400 MHz).

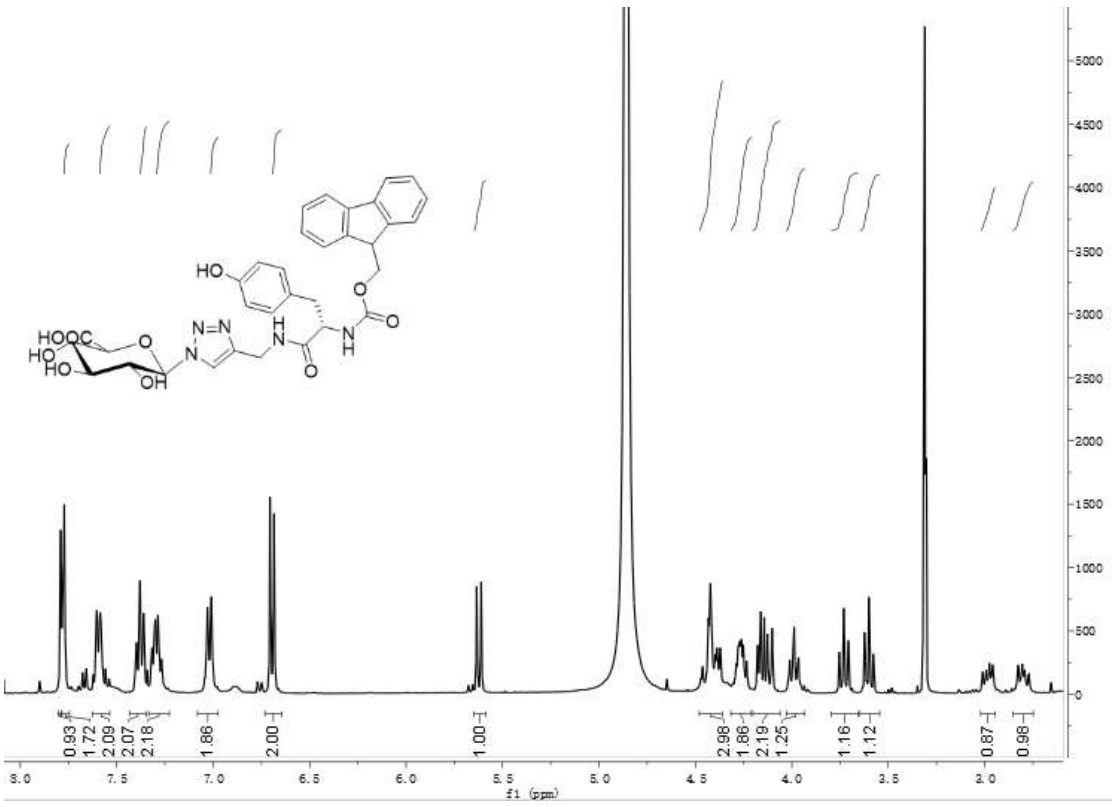

Figure S17. ^{1}HNMR spectrum of **GlcA-YF** (DMSO-d_6, 400 MHz).

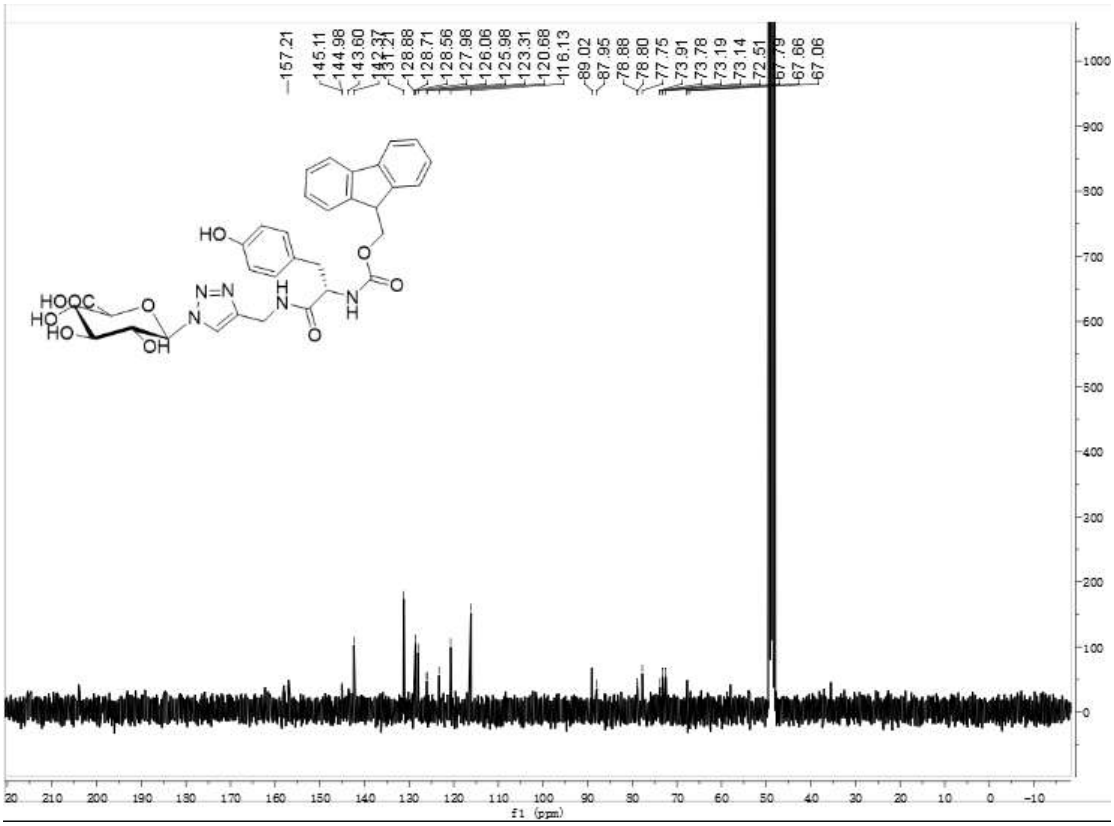

Figure S18. ^{13}C NMR spectrum of **GlcA-YF** (DMSO-d_6, 100 MHz).

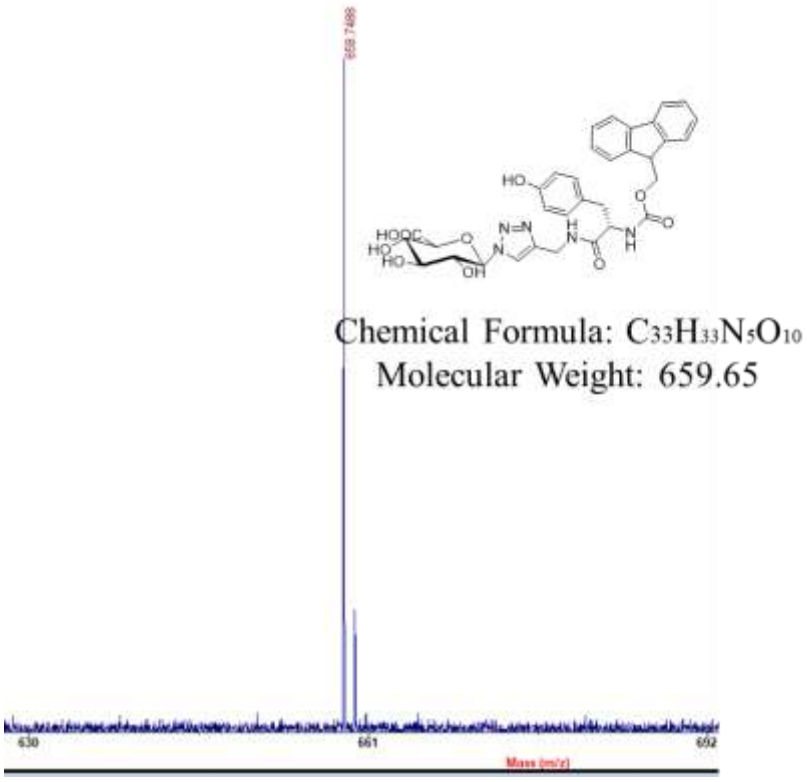

Figure S19. Maldi-TOF MS spectrum of **GlcA-YF**

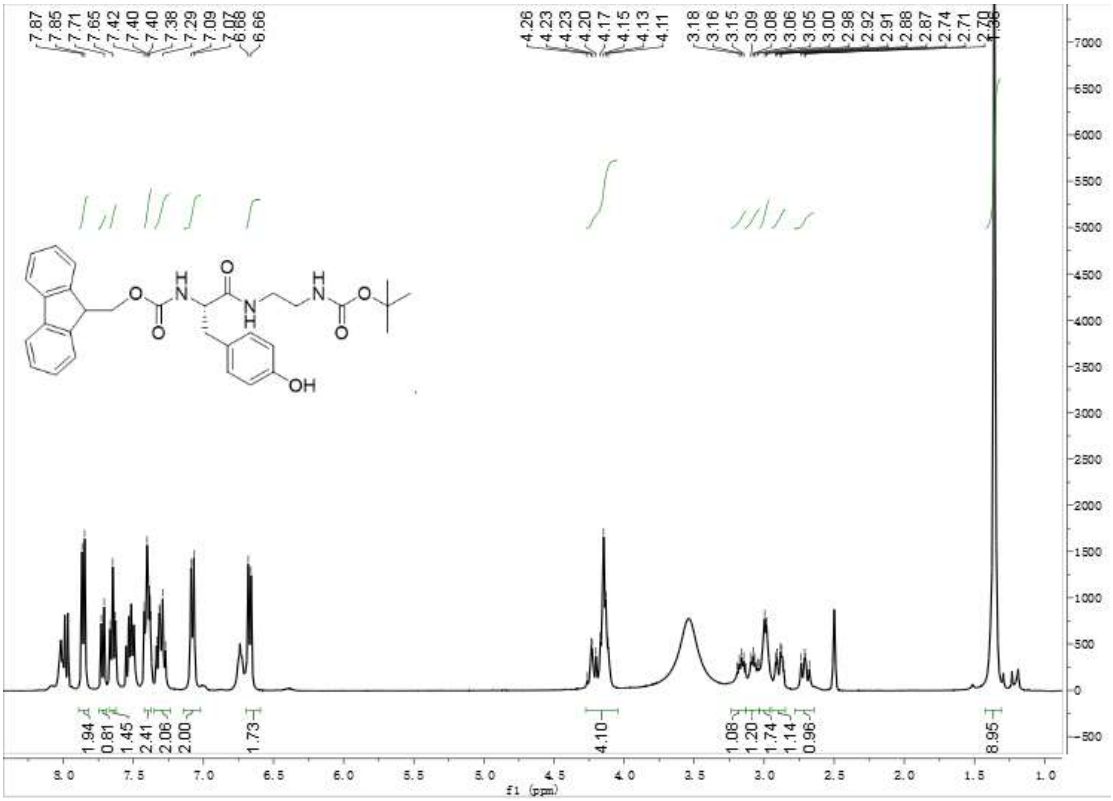

Figure S20. ^{1}H NMR spectrum of **S3** (DMSO-d_6, 400 MHz).

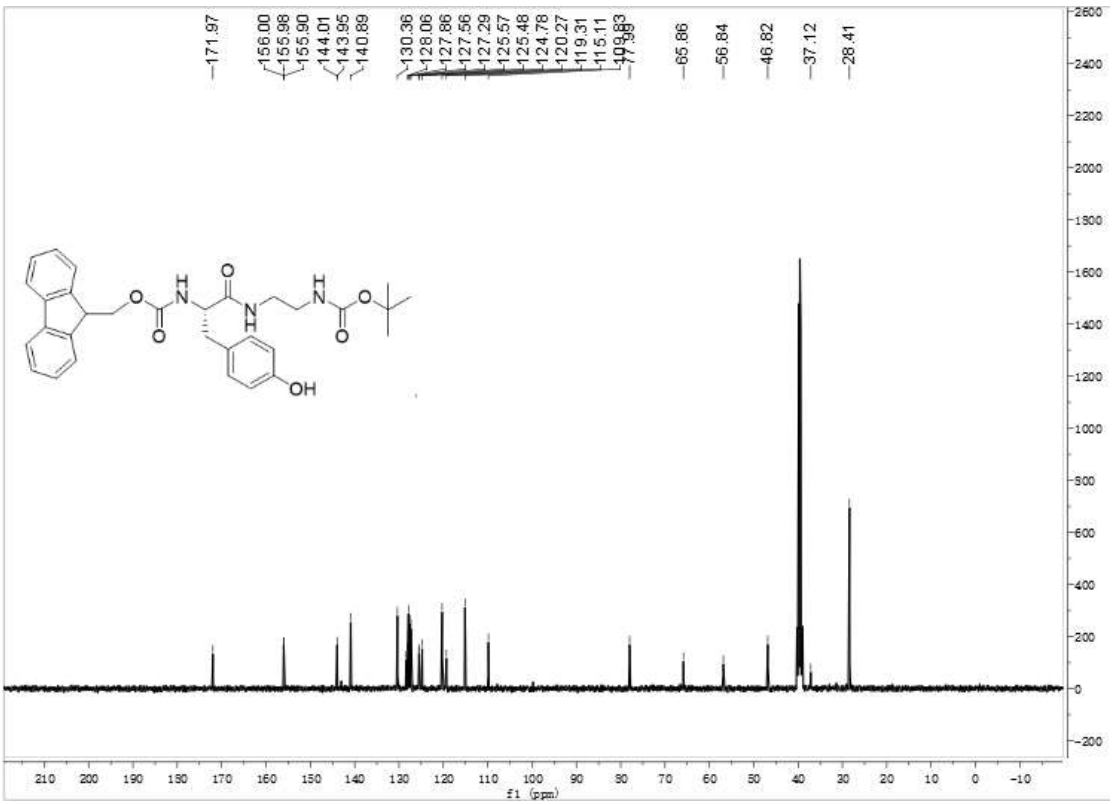

Figure S21. ^{13}C NMR spectrum of **S3** (DMSO-d_6, 100 MHz).

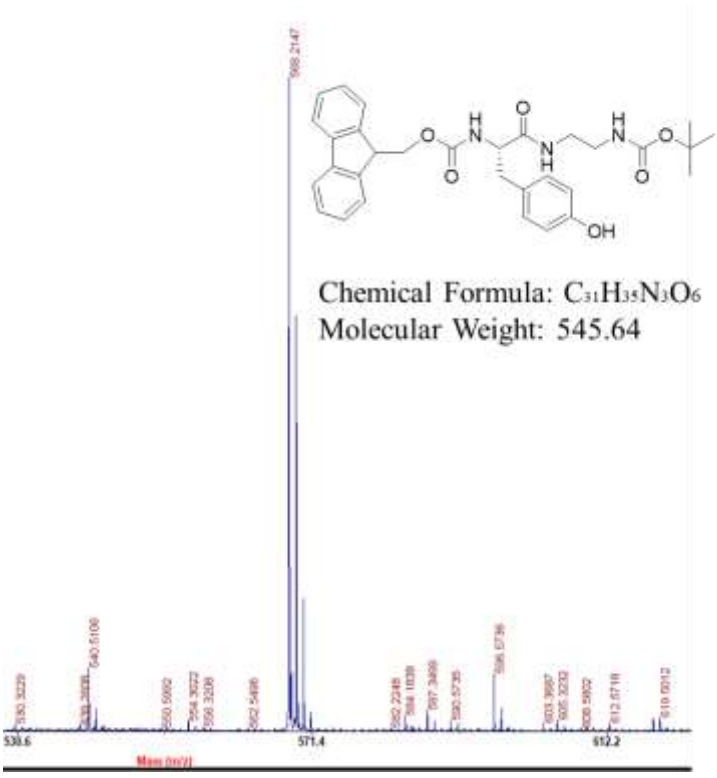

Figure S22. Maldi-TOF MS spectrum of **S3**.

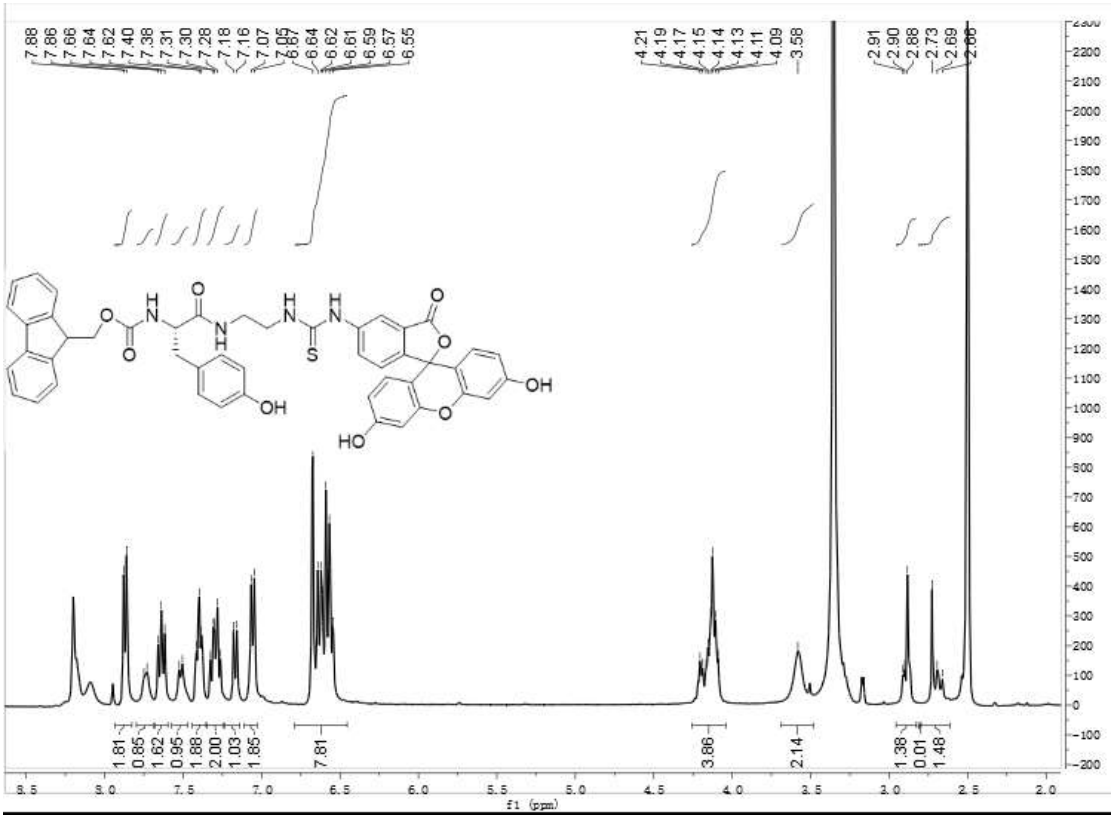

Figure S23. ^{1}H NMR spectrum of **FITC-YF** (DMSO-d_6, 400 Hz).

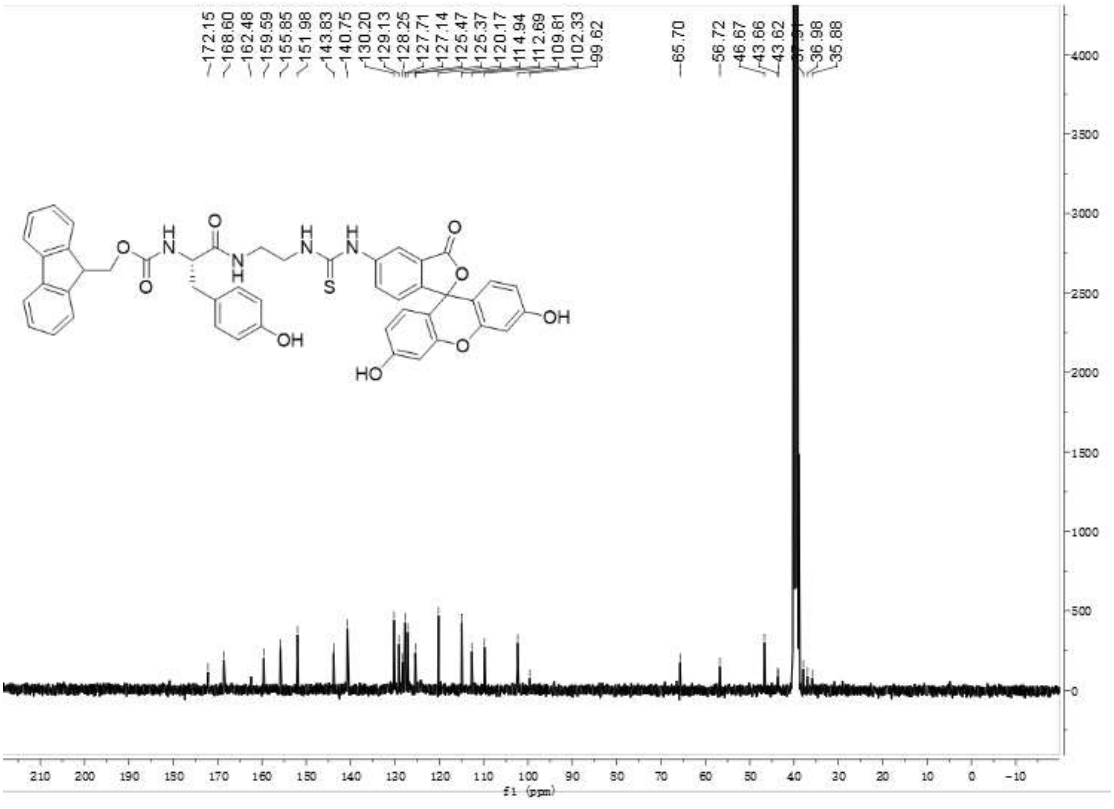

Figure S24. ^{13}C NMR spectrum of **FITC-YF** (DMSO-d_6, 100 MHz).

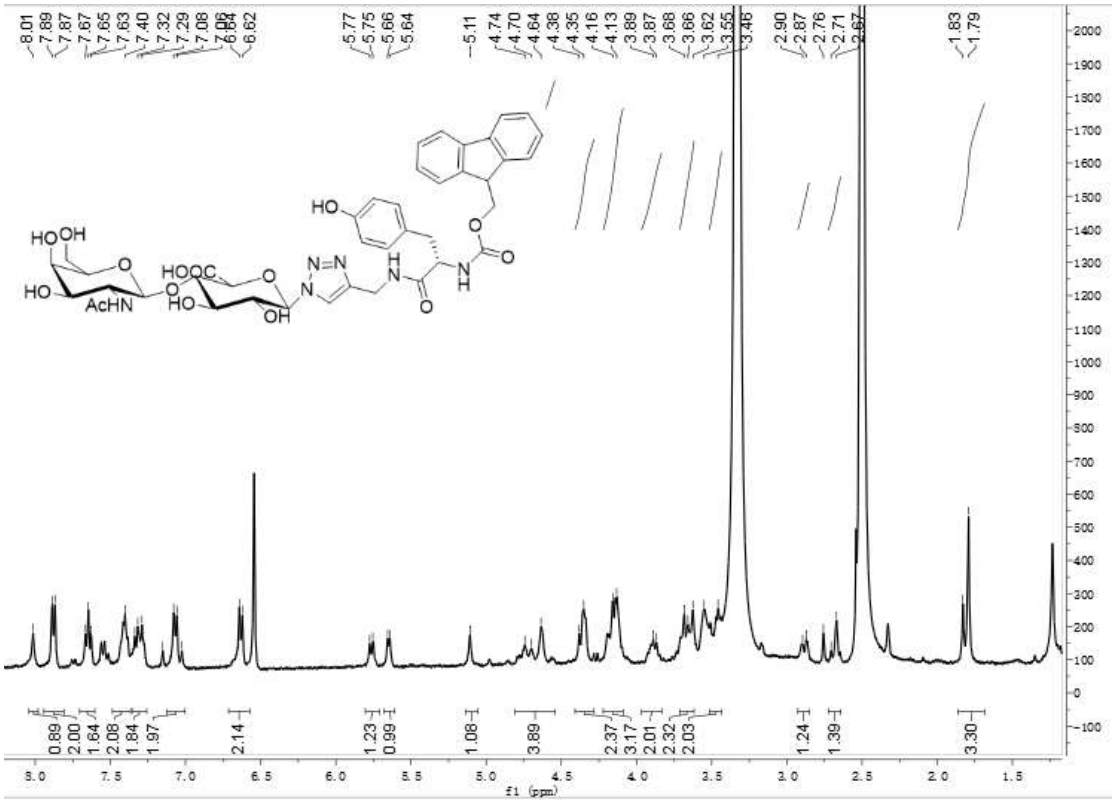

Figure S25. ^{1}H NMR spectrum of **GalNAcGlcA-YF** (DMSO-d_6, 400 MHz).

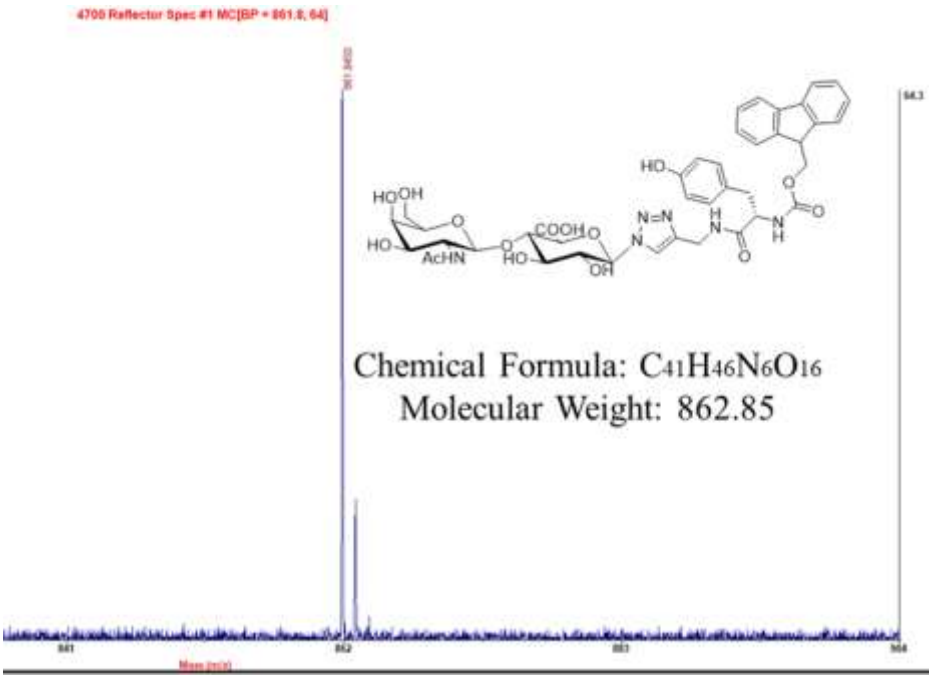

Figure S26. Maldi-TOF MS spectrum of **GalNAcGlcA-YF**.

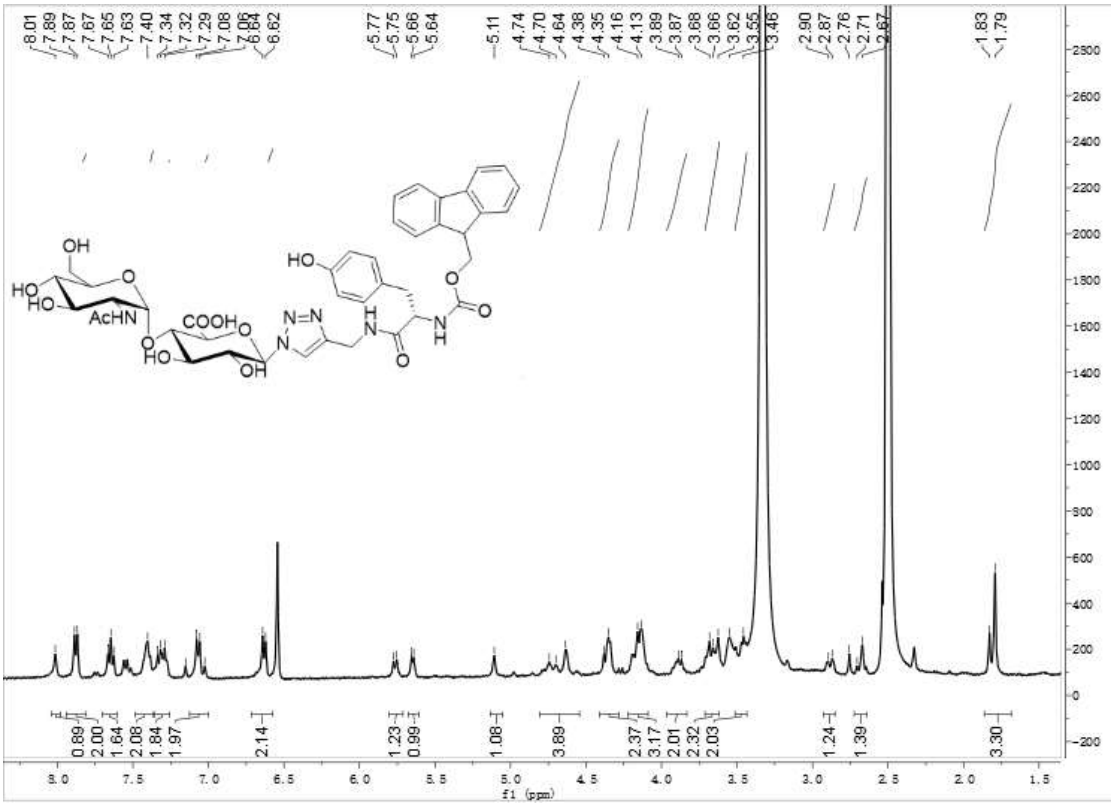

Figure S27. ^{1}H NMR spectrum of **GlcNAcGlcA-YF** (DMSO-d_6, 400 MHz).

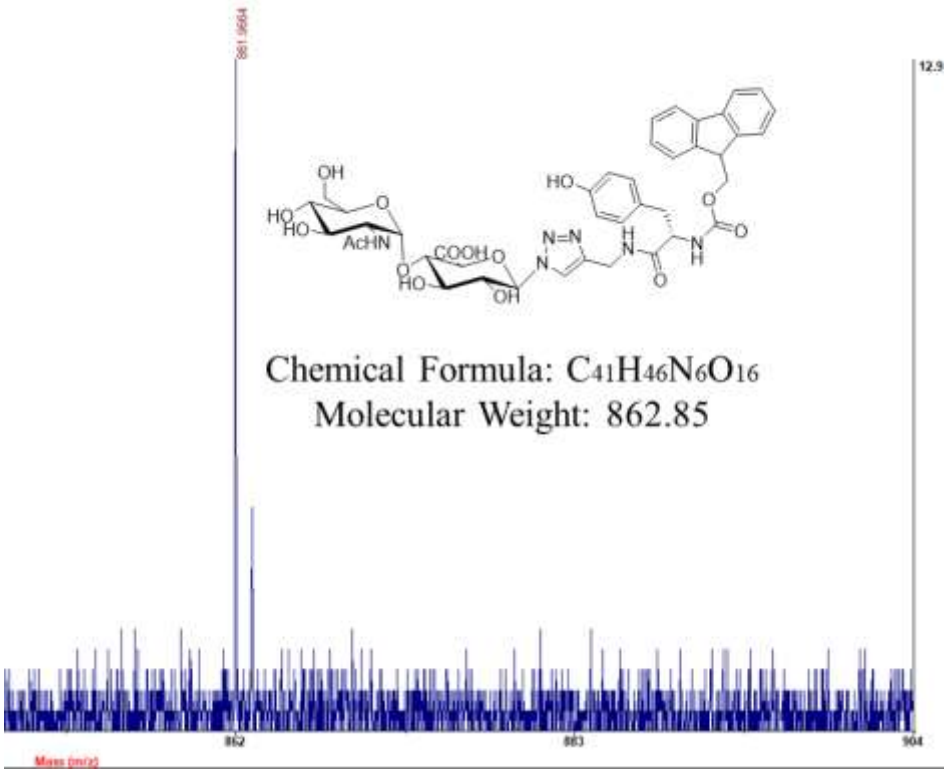

Figure S28. Maldi-TOF MS spectrum of **GlcNAcGlcA-YF**.

XI. Reference

[1] Tanaka, J.; Gleinich, A. S.; Zhang, Q.; Whitfield, R.; Kempe, K.; Haddleton, D. M.; Davis, T. P.; Perrier, S; Mitchel, D. A. Specific and Differential Binding of N-Acetylgalactosamine Glycopolymers to the Human Macrophage Galactose Lectin and Asialoglycoprotein Receptor. *Biomacromolecules* **2017**, *18* (5), 1624-1633.

[2] Xue, J.; Jin, L.; Zhang, X.; Wang, F.; Lin, P.; Sheng, J. Impact of donor binding on polymerization catalyzed by KfoC by regulating the affinity of enzyme for acceptor. *BBA-GEN SUBJECTS*. **2016**, *1860* (4), 844–855.